

Nudol, a phenanthrene derivative from *Dendrobium nobile*, induces cell cycle arrest and apoptosis and inhibits migration in osteosarcoma cells

This article was published in the following Dove Press journal:
Drug Design, Development and Therapy

Yuying Zhang¹
Qianqian Zhang¹
Wei Xin²
Na Liu¹
Hua Zhang¹

¹School of Biological Science and Technology, University of Jinan, Jinan, People's Republic of China; ²Central Laboratory, Shandong Provincial Hospital, Shandong University, Jinan, People's Republic of China

Purpose: Osteosarcoma is the most common malignancy of the bone in children and adolescents. There is an urgent need for the development of novel drugs to treat it. Nudol (1), a phenanthrene compound from the traditional Chinese medicine, *Dendrobium nobile*, exhibited antiproliferative activity against osteosarcoma cells. Therefore, the aim of the present study was to investigate the role and underlying mechanism of nudol(1) as potential chemotherapy for osteosarcoma.

Methods: Cell viability was determined by MTT assay. Cell-cycle phase distribution was analyzed by flow cytometry and Western blot. DAPI staining was used for morphology observation. Apoptosis was analysis via flow cytometry. The expression levels of mRNA and protein related to capase-mediated apoptotic pathway were detected by real-time PCR and western blotting. Migration was determined by wound healing assays.

Results: Nudol(1) significantly decreased cell viability in several cancer cell lines. Moreover, nudol(1) caused cell cycle arrest at G2/M phase in U2OS cells, and it also induced cell apoptosis through the caspase-dependent pathway. In addition, treatment with nudol(1) suppressed the migration of U2OS cells.

Conclusion: The present study, for the first time, demonstrated effects of nudol(1) on OS in vitro and the potential molecular mechanisms. Accordingly, nudol(1) might have the potential for further development as a lead compound against bone tumor.

Keywords: nudol(1), phenanthrene, *Dendrobium nobile*, anti-proliferation, osteosarcoma

Introduction

Osteosarcoma is the most common malignant bone tumor, particularly in children, adolescents, and young adults.¹ Pathologically, osteosarcoma is derived from mesenchymal cells which are characterized by spindle cells and aberrant osteoid formation. The primary sites of osteosarcoma are typically located at the proximal tibia, the distal femur, and the distal humerus, with about 60% lesions arising from the knee.² Traditional therapeutic approaches for osteosarcoma include local control of the primary lesion by surgery and/or chemotherapy, and treatment of disseminated disease with multi-agent cytotoxic chemotherapy.³ However, the current five-year survival rate for patients with osteosarcoma is only 5%–20%,⁴ and a significant proportion of osteosarcoma cases has shown strong resistance to the present chemotherapies. Consequently, development of new, more effective, and well-tolerated therapeutics remains a pressing task.

Medicinal plants are important sources of novel therapeutic drugs for the treatment of osteosarcoma.⁵ Many species of the genus *Dendrobium* Sw. (family

Correspondence: Na Liu; Hua Zhang
School of Biological Science and Technology, University of Jinan, 336 West Road of Nan Xinzhuang, Jinan 250022, People's Republic of China
Tel +86 5 318 973 6199
Email mls_liun@ujn.edu.cn;
bio_zhangh@ujn.edu.cn

Orchidaceae) have been used for over 1,000 years as first-rate herbs in traditional Chinese medicine (TCM).⁶ A number of bioactive constituents from *Dendrobium* plants, such as polysaccharides,⁷ bibenzyls,⁸ phenanthrenes,⁹ and alkaloids¹⁰ were obtained and displayed diverse pharmacological effects including anticancer, anti-diabetic, neuroprotective, and immunomodulating activities. The most noteworthy constituent is erianin, which is a natural bibenzyl compound derived from *Dendrobium chrysotoxum* Lindl and has been used as an analgesic in TCM.¹¹ Previous studies have proved the antitumor activity of erianin against a panel of human cancer cell lines, including breast cancer T47D,¹² promyelocytic leukemia HL-60,¹³ patocarcinoma Bel7402 and melanoma A375,¹⁴ and osteosarcoma cells.¹⁵ Structurally similar to erianin, some phenanthrene derivatives were also found to display potent antitumor activity.^{16–19} The latest study demonstrated that chrysotoxene induced the apoptosis of HepG2 cells in vitro and in vivo via activation of the mitochondria-mediated apoptotic signaling pathway.²⁰

During the course of our search for bioactive natural products from *Dendrobium nobile* Lindl., five phenanthrene derivatives were isolated and structurally characterized as nudol(1),²¹ confusarin (2),²² 3,7-dihydroxy-2,4-dimethoxy-9,10-dihydrophenanthrene (3),²³ 3,7-dihydroxy-2,4-dimethoxyphenanthrene (4),²⁴ and 3,7-dihydroxy-2,4,8-trimethoxyphenanthrene (5)²⁵ (Figure 1) (Figures S4–S13). Among them, nudol(1) was initially isolated from the orchids *Eulophia nuda* Lindl, *Eria carinata* Gibson, and *Eria stricta* Lindl,²¹ and significantly inhibited the growth of HeLa cells ($IC_{50}=20.18 \mu\text{M}$).²⁶ A preliminary screening of the anti-proliferative activity of 1–5 against osteosarcoma cells MG63 and U2OS revealed that nudol(1) exerted remarkable growth inhibitory effect (Figure 2). Therefore, the aim of the present work

was to perform an antitumor evaluation of nudol(1) toward the osteosarcoma cells and to investigate the critical factors for the cell growth inhibition including cell cycle, apoptosis, and migration.

Materials and methods

General experimental procedures

NMR spectra were acquired on a Bruker Avance DRX600 NMR spectrometer (Bruker BioSpin AG) with residual solvent peaks as references (CDCl_3 ; δ_{H} 7.26, δ_{C} 77.0). Semi-preparative HPLC separations were carried out on an Agilent 1260 series (Agilent Technologies Inc.) using an Agilent Zorbax SB-C₁₈ column (250×9.4 mm, 5 μm). ESIMS analyses were carried out on an Agilent 1,260–6,460 Triple Quad LC-MS instrument (Agilent Technologies Inc.). Column chromatography (CC) was performed on Silica gel (200–300 mesh, Yantai Jiangyou Silica Gel Development Co.), reversed phase (RP) C18 silica gel (Merck) and Sephadex LH-20 gel (GE Healthcare Bio-Sciences). All solvents used for CC were of analytical grade (Tianjin Fuyu Fine Chemical Co. Ltd.), and solvents used for HPLC were of HPLC grade (Oceanpak Alexative Chemical Ltd.).

Plant material

The stems of *Dendrobium nobile* were purchased in April 2015 from Huoshan, Anhui Province, and were authenticated by Dr. Jinchuan Zhou from School of Pharmacy, Linyi University. A voucher specimen (No. DN20150420) has been preserved at School of Biological Science and Technology, University of Jinan.

Extraction and isolation

The air-dried and powdered stems (2.5 kg) of *D. nobile* were extracted with 95% EtOH (3×10 L, each for 5 days)

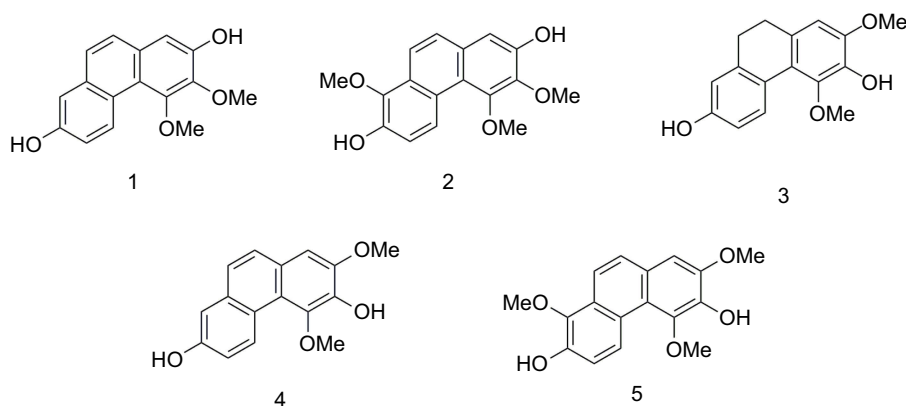


Figure 1 Chemical structures of compounds 1–5.

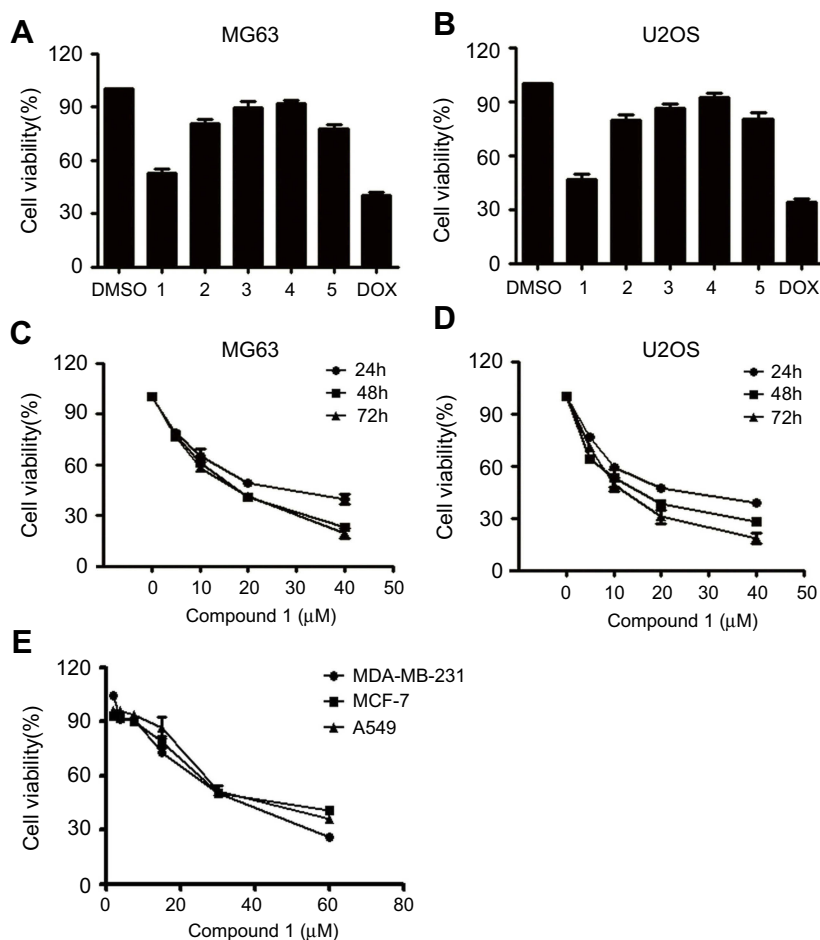


Figure 2 Effects of tested compounds on cell viability.

Notes: (A, B) U2OS and MG63 cells were treated with 20 μ M compounds for 24 hrs, and cell viability was determined by MTT assay; DOX (20 nM) was used as a positive control. (C, D) Osteosarcoma cell viability by treatment with various concentrations of nudol(1) for 24, 48, and 72 hrs. (E) MDA-MB-231, MCF-7, and A549 cell viability following treatment with the various concentrations of nudol(1) for 48 hrs. Data were expressed as mean \pm SD. * $P < 0.05$; ** $P < 0.01$ vs control cells.

Abbreviations: MTT, 3-(4,5-dimethylthiazol-2-yl)-2,5-diphenyltetrazolium bromide; DOX, doxorubicin hydrochloride.

at room temperature. After concentration under reduced pressure, the crude residue (180.3 g) was suspended in H_2O (1.0 L) and partitioned with EtOAc (0.5 L \times 3). The EtOAc extract (95.2 g) was subjected to silica gel CC and eluted with gradient petroleum ether-acetone (200:1–1:1) to afford six fractions (Fr. 1–6). Fr. 3 (1.2 g) was first chromatographed on a Sephadex LH-20 column (MeOH- $CHCl_3$, 1:1) and then separated by an RP-18 silica gel column (MeOH- H_2O , 5:5 to 9:1) to yield four subfractions (Fr. 3.1–3.4). Fr. 3.2 (30.2 mg) was purified by HPLC (MeOH- H_2O , 60:40, 2.0 mL/min) to yield 1 (2.4 mg, $t_R = 20.4$ mins, purity 96.2%) and 2 (2.6 mg, $t_R = 23.7$ mins). Fraction 4 (1.9 g) was subjected to silica gel CC and eluted with gradient petroleum ether-acetone (100:1–5:1) to generate five subfractions (Fr. 4.1–4.5). Fr. 4.3 (260 mg) was further separated on a Sephadex LH-20 column (MeOH- $CHCl_3$, 1:1), followed by purification on HPLC (MeOH- H_2O , 70:30, 2.0 mL/min) to afford 3 (8.1 mg, $t_R = 33.2$

mins), 4 (6.9 mg, $t_R = 34.6$ mins), and 5 (13.4 mg, $t_R = 45.9$ mins).

Cell culture

Cell lines MCF-7, MDA-MB-231, A549, U2OS, and MG63 were acquired from the Cell Bank of Chinese Academy of Sciences (Shanghai, China). All the cells were cultured in high-glucose Dulbecco's Modified Eagle's Medium (Thermo, Waltham, MA, USA) supplemented with 10% fetal bovine serum (Gibco), 100 IU/mL penicillin, and 100 μ g/mL streptomycin (both from Thermo Fisher Scientific Inc) in a humidified atmosphere containing 5% CO_2 at 37°C. The phenanthrene derivatives (1–5) were initially dissolved DMSO (dimethylsulfoxide) to make a 20 mM stock solution and diluted with culture media to the final test concentrations, which contained no more than 0.05% DMSO. Doxorubicin hydrochloride

(DOX, Sigma Chemical Co, purity >98%) was dissolved in distilled water and used as a positive control.

Cell viability assay

The cells were cultured in 96-well plates, and each well was seeded with 1×10^4 cells. The viability of cells was measured by the 3-(4,5-dimethylthiazol-2-yl)-2,5-diphenyltetrazolium bromide (MTT) assay. Briefly, 10 μ L of MTT (5 mg/mL in PBS) was added to each well, and the plates were incubated for 4 hrs at 37°C. In this step, 100 μ L of DMSO was added to dissolve the formazan crystals. The optical density was measured at an absorbance wavelength of 490 nm using a Microplate Reader (Tecan). The survival rate was calculated according to the following formula: Survival rate = absorbance of treatment/absorbance of control $\times 100\%$.

DNA fragmentation analysis with DAPI staining

Cells (1×10^5 cells/well) were seeded in six-well plates. After attachment, cells were treated with various concentrations of nudol(1) for 48 hrs. The cells were then fixed with 4% polyoxymethylene (PFA, Sigma-Aldrich) for 30 mins, washed twice with PBS, and incubated with 10 μ g/mL DAPI (4,6-diamidino-2-phenylindole, Sigma-Aldrich) for 10 mins at room temperature in the dark. After washing with PBS two times, the images were photographed by an inverted fluorescence microscope (Leica).

Apoptosis analysis by flow cytometry

Cell apoptosis assays were performed with an Annexin V-FITC apoptosis detection kit (BD Biosciences) according to the manufacturer's protocol. OS cells were treated with different doses of nudol(1) for 48 hrs. Cells were washed twice with PBS and harvested by re-suspension in 100 μ L of $1 \times$ binding buffer, followed by incubation with 5 μ L each of Annexin V fluorescein isothiocyanate and propidium iodide for 15 mins at room temperature in the dark. Finally, adding 400 μ L of $1 \times$ binding buffer to the tube and cell apoptosis was measured by flow cytometer (Becton-Dickinson). The data were analyzed using Flowjo 7.0.

Cell cycle analysis by flow cytometry

Cells were incubated with the indicated concentrations of nudol(1) for 48 hrs. After incubation, cells were collected, washed twice with PBS, and then fixed in cold 70% ethanol overnight at 4°C. The cells were then again

washed in PBS once and suspended in a staining buffer (10 μ g/mL propidium iodide, 0.5% Tween 20, 0.1% RNase in PBS) for 30 mins at room temperature. Cell cycle analysis was performed on the flow cytometer (Becton-Dickinson).

Migration determination

Cell migration was determined by wound-healing assay. The cells were seeded at a density of 5×10^5 cells/well in six-well plates. After the cell monolayer was formed, a micropipette tip was used to create wounds. The cells were then washed with PBS and replaced by serum-free DMEM-high glucose medium containing various concentrations of nudol(1). The cell migration progress into the wound area was photographed using an inverted microscope at 0, 6, 18, and 24 hrs. The average wound size represented the relative cell migration.

Reverse transcription and quantitative real-time PCR

Total RNA of U2OS cells treated with or without nudol(1) for 48 hrs was extracted using TRIzol reagent (Invitrogen) according to the manufacturer's protocol. The quantity of RNA was determined using the ultramicro spectrophotometer (NanoDrop 2,000, Thermo Fisher Scientific). Complementary DNA was generated in a 20 μ L reaction with 1 μ g of total RNA using a RT reaction kit (Promega) according to the manufacturer's instruction. Real-time PCR was performed using a CRX Connect Real-Time system (Bio-Rad) and using SYBR Premix Ex Taq™ (TaKaRa) as a DNA-specific fluorescent dye. Real-time PCR was carried out for 40 cycles at 95°C for 10 s and 60°C for 30 s. Gene expression levels were calculated relative to the housekeeping β -actin, and all the reactions were repeated at least three times. Primer sequences for detection of mRNA expression were synthesized as shown in Table 1.

Western blot analysis

The U2OS cells were treated with the different doses of nudol(1) for 48 hrs. The cells were then washed twice with PBS solution, and total proteins were extracted from cells using $1 \times$ RIPA buffer containing protease/phosphatase inhibitor (Beyotime Institute of Biotechnology, Jiangsu, China). The U2OS cells were prepared using a ProteoJET cytoplasmic protein extraction kit (Fermentas; Thermo Fisher Scientific, Inc.). Protein concentrations

Table 1 The primers of real-time PCR

Name	Forward primer (5'-3')	Reverse primer (5'-3')
Bax	AGCTGAGCGAGTGTCTCAAG	GTCCAATGTCCAGCCCATGA
Bcl-2	GGTGAAGTGGGGGAGGATTG	GGCAGGCATGTTGACTTCAC
Caspase-3	TGTGAGGCGGTTGTAGAAGTT	GCTGCATCGACATCTGTACC
Caspase-9	TCCCCAGGTTTTGTTTCTG	CCTTTCACCGAAACAGCATT
Caspase-8	CATCCAGTCACTTTGCCAGA	GCATCTGTTTCCCCATGTTT
Cytochrome c	GAGATGAACAGGGGCTCGAAC	TGCTTCTGCCACATGATAACGAG
CDK1	CTGGCTGATTTGGCCTTGC	CCACTTCTGGCCACACTTCA
CDK2	TTTGCTGAGATGGTACTCG	CCTCATCCAGGGGAGGTACA
CDK4	TGAGGGGGCCTCTAGCTT	TGAGGGGGCCTCTAGCTT
CDK10	TGGACAAGGAGAAGGATG	CTGCTCACAGTAACCCATC
MMP2	GAGTGCATGAACCAACCAGC	GTGTTTCAGGTATTGCATGTGCT
MMP9	CCTTGAGTCCGGTGGACGAT	TCGCCAGTACTTCCCATCCT
TIMP1	GCAATTCGGACCTCGTCATC	TAGACGAACCGGATGTCAGC
TIMP2	CTGCGAGTGCAAGATCACG	TGGTGCCCGTTGATGTTCTT
β -actin	GCCGCCAGCTCACCAT	TCGATGGGGTACTTCAGGGT

Abbreviations: CDK, cyclin-dependent kinases; MMP, matrix metalloproteinase; TIMP, tissue inhibitor of metalloproteinase.

were determined using BCA protein assay kit (Beyotime Institute of Biotechnology, Jiangsu, China). Equivalent quantities of protein were electrophoretically separated on a 10% sodium dodecyl sulfate-polyacrylamide gel. The total protein were then transferred onto polyvinylidene fluoride membranes and blocked for 60 mins with 3% bovine serum albumin solution prepared in PBS at room temperature. A 1:1,000 dilution of the primary antibodies (Bax, Bcl-2, caspase-3, caspase-9, caspase-8, CDK1, cyclinE1, cyclinD1, cyclinB1, p21, p-Rb, cytochrome c, and β -actin) were incubated overnight at 4°C. The membranes were washed three times with TBST buffer (0.05% Tris-buffered saline and Tween 20). The appropriate peroxidase-conjugated secondary antibody (dilution of 1:5,000) was incubated for 2 hrs at room temperature. Subsequently, the results were visualized with enhanced chemiluminescence reagent (Merck Millipore) using imaging system (Chemi-Doc XRS imager, Bio-Rad).

Statistical analysis

All experimental values were expressed as mean \pm standard deviation (SD) of at least three independent experiments. SPSS 18.0 statistical software package (SPSS Inc) was used to perform all statistical analysis. The statistical significance of the differences between groups was evaluated by Student's *t*-test. $P < 0.05$ was considered to indicate a statistically significant difference. * $p < 0.05$, ** $p < 0.01$, and *** $p < 0.001$, respectively.

Results

Nudol(1) decreased the cell viability of osteosarcoma cells

Compounds 1–5 were initially evaluated for their anti-proliferative activity against the human osteosarcoma cell lines U2OS and MG63 at 20 μ M, using MTT assay. The results were shown in Figure 2A and B, and nudol(1) exhibited obvious anti-proliferative activity against both cells. To further investigate the effect of nudol(1) on cell proliferation, MG63 and U2OS cells were treated by various concentrations of nudol(1) for 24, 48, and 72 hrs. We found that nudol(1) decreased osteosarcoma cell viability in dose- and time-dependent manners (Figure 2C and D). The IC_{50} values were $21.86 \pm 0.17 \mu$ M (24 hrs), $14.58 \pm 0.24 \mu$ M (48 hrs), and $12.97 \pm 0.28 \mu$ M (72 hrs) for MG63 cell line, while those for U2OS cell line were $21.52 \pm 0.08 \mu$ M (24 hrs), $13.99 \pm 0.16 \mu$ M (48 hrs), and $11.29 \pm 0.21 \mu$ M (72 hrs). At the same time, the viability effect of nudol(1) was examined on the other human cancer cell lines by the MTT assay. Treatment with nudol(1) for 48 hrs inhibited the growth of MDA-MB-231, MCF-7, and A549 cancer cells in a dose-dependent manner with the IC_{50} values of 30.05 ± 0.2 , 38.27 ± 0.23 , and $37.45 \pm 0.26 \mu$ M, respectively (Figure 2E). These results demonstrated that U2OS cells showed the lowest IC_{50} value among the cancer cell lines tested. Therefore, we further examined the effect of nudol(1) on the U2OS cells.

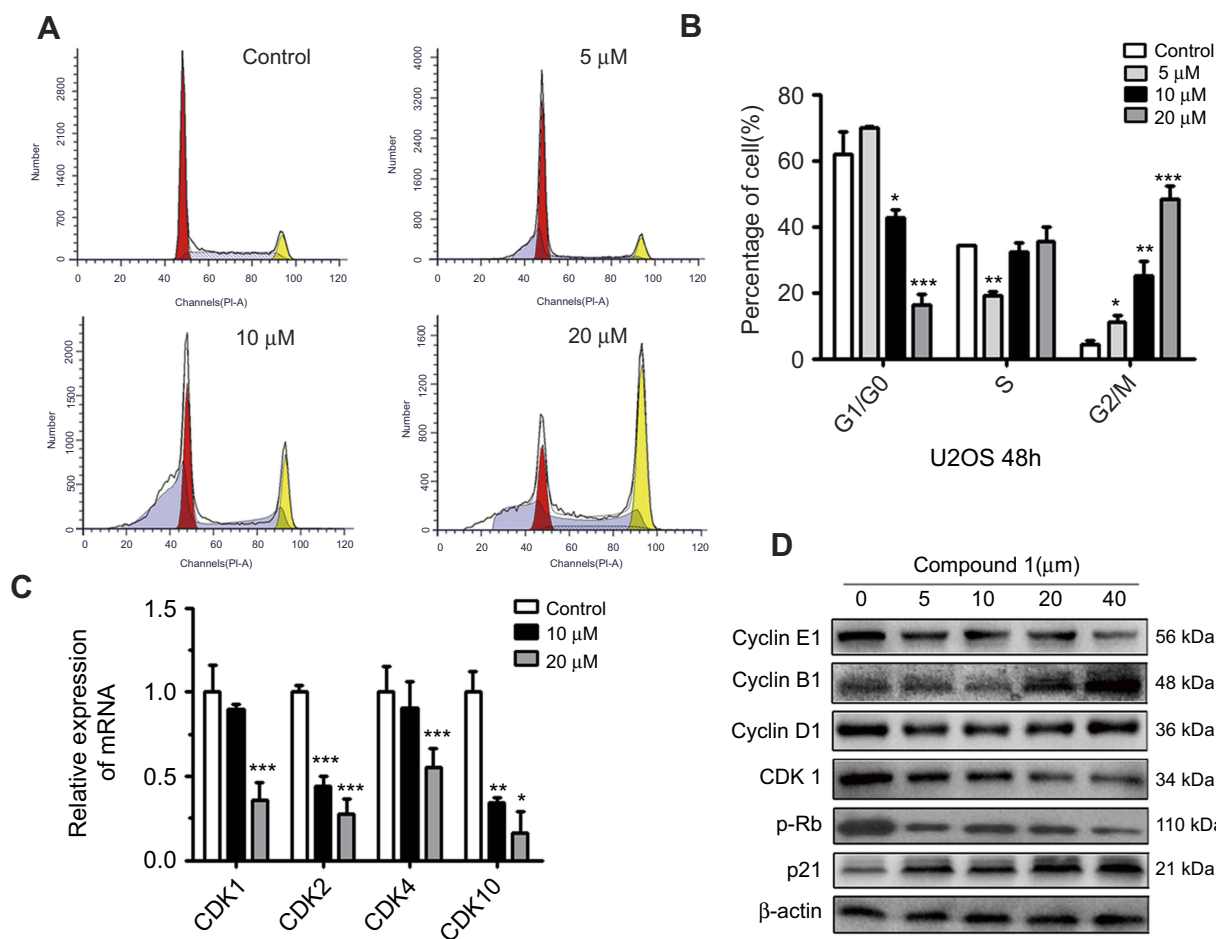


Figure 3 Nudol(1) induced cell cycle arrest at G2/M phase.

Notes: (A, B) U2OS cells were treated with nudol(1) for 48 hrs. The distribution of cell cycle was assessed by flow cytometry. The percentage of cells in each phase was shown as mean \pm SD (n=3). (C and D) U2OS cells were exposed to nudol(1) for 48 hrs. The expression of cell cycle-regulated genes was analyzed by real-time PCR and Western blotting, respectively. * $P < 0.05$, ** $P < 0.01$, and *** $P < 0.001$ vs vehicle control.

Abbreviation: Rb, retinoblastoma tumor suppressor protein.

Nudol(1) induced cell cycle arrest at G2/M phase in OS cells

To verify how treatment of nudol(1) caused the inhibition of U2OS cell proliferation, cell-cycle distribution was analyzed by flow cytometry (Figure 3A and B). Nudol(1) increased the cell number at G2/M phase after 48 hrs treatment with different concentrations, while the percentage of cells in G1 phase decreased significantly. The results indicated that nudol(1) effectively arrested the cell cycle at G2/M phase compared to the control group. In addition, we explored the effects of nudol(1) on cell cycle in MG63 cells. Results further confirmed that nudol(1) caused cell cycle arrests at G2/M phase (Figure S1).

To study the molecular mechanisms of how nudol(1) induced G2/M phase arrest, the cell cycle arrest-related cyclin-dependent kinases (CDK) family transcriptional

level was examined using the real-time PCR. The results displayed that treatment of nudol(1) prominently decreased the transcription of CDK1, CDK2, CDK4, and CDK10 compared to the control group (Figure 3C). Furthermore, the expression of cell cycle-related proteins in response to treatment of nudol(1) was measured by Western blotting. The expression of Cyclin B1 and p21 (DNA synthesis inhibitor) was up-regulated, and the level of CDK1 and p-Rb was down-regulated (Figure 3D). All these observations demonstrated that nudol(1) triggered G2/M phase arrest by regulating cell cycle-related proteins.

Nudol(1) induced apoptosis of OS cells

We next investigated whether the reduction of cell viability by nudol(1) treatment was due to the induction of apoptosis, and DAPI staining assay was thus carried out.

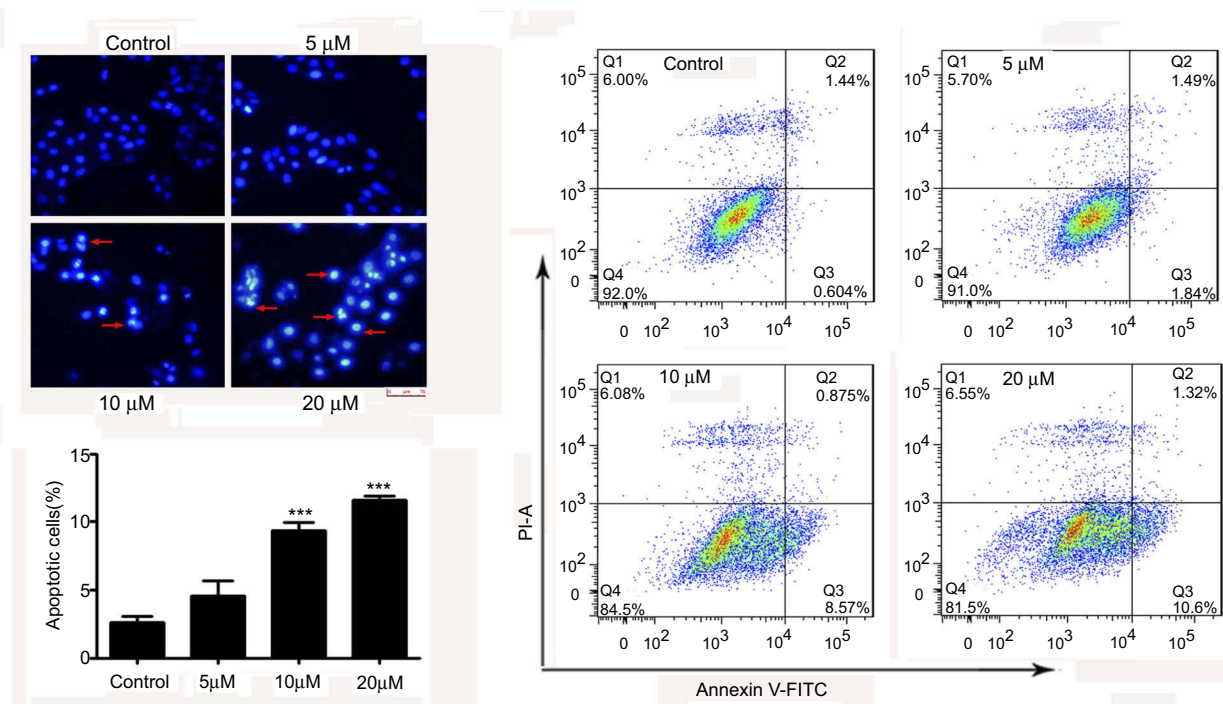


Figure 4 Nudol(1) induced cell apoptosis.

Notes: (A) U2OS cells were treated with nudol(1) for 48 hrs and subjected to DAPI staining, and were then viewed under a fluorescent microscope at the magnification of 200. Arrows indicate apoptotic characteristics of treated cells. (B) Apoptosis was determined by an annexin V-FITC/PI apoptosis detection kit, and representative results from flow cytometry were shown. (C) Quantitative analysis of apoptosis of U2OS cells as shown in (B). Values were presented as mean \pm SD (n=3). *** P <0.001 vs normal control.

Abbreviations: DAPI, 4,6-diamidino-2-phenylindole; annexin V-FITC, annexin V fluorescein isothiocyanate.

Treatment of nudol(1) for 48 hrs increased the number of hallmarks of U2OS cell apoptosis in a concentration-dependent manner, including pyknosis (shrinkage) and condensed chromatin (brighter nuclei) (Figure 4A). We then analyzed U2OS cell line by flow cytometry after staining with Annexin V-FITC and propidium iodide (Figure 4B). Similar results showed (Figure 4C) that treatment with nudol(1) increased the percentage of apoptotic cells from $2.58 \pm 0.50\%$ (control) to $11.59 \pm 0.29\%$ (20 μ M). Furthermore, flow cytometric analysis via Annexin V-FITC/PI was performed on MG63 cell. We also found that an increase of the number of apoptotic cells was observed in cells after exposed to nudol(1) in a dose-dependent manner (Figure S2). These results were consistent with the cell viability assay, suggesting that higher cell growth inhibition resulting from nudol(1) could be, at least partly, due to the induction of more apoptosis in U2OS cells.

Nudol(1) induced cell apoptosis through caspase pathway

In an attempt to clarify the detailed molecular mechanism involved in apoptosis induction, we proceeded to

assess the expression levels of caspase-3, 8, and 9, and modulation of the status of other apoptosis-related genes. The mRNA levels of caspase-3, 8, and 9 in the application of 20 μ M nudol(1) were much higher than the control (Figure 5A). Furthermore, release of cytochrome c into cytosol is a key step in apoptotic process, as shown in Figure 5A and C, the mRNA and protein of cytochrome c was obviously increased in the experimental group. Subsequently, the effect of nudol(1)-treatment on caspase-3, 8, and 9 activities in U2OS cells was investigated (Figure 5B). Western blotting revealed that nudol(1) significantly induced the cleaved forms of caspase-3, 8, and 9 of U2OS cells at 48 hrs, illustrating the activation of both extrinsic and intrinsic apoptosis pathways.

Further experiments were done to examine the key players in apoptosis pathway such as Bax and Bcl-2. As shown in Figure 5D and E, the level of anti-apoptotic Bcl-2 was down-regulated, which was accompanied by an increased level of pro-apoptotic Bax in response to treatment with nudol(1). These results provided insight into the molecular mechanism of how compound nudol(1) exerted its growth inhibitory effects on osteosarcoma cells.

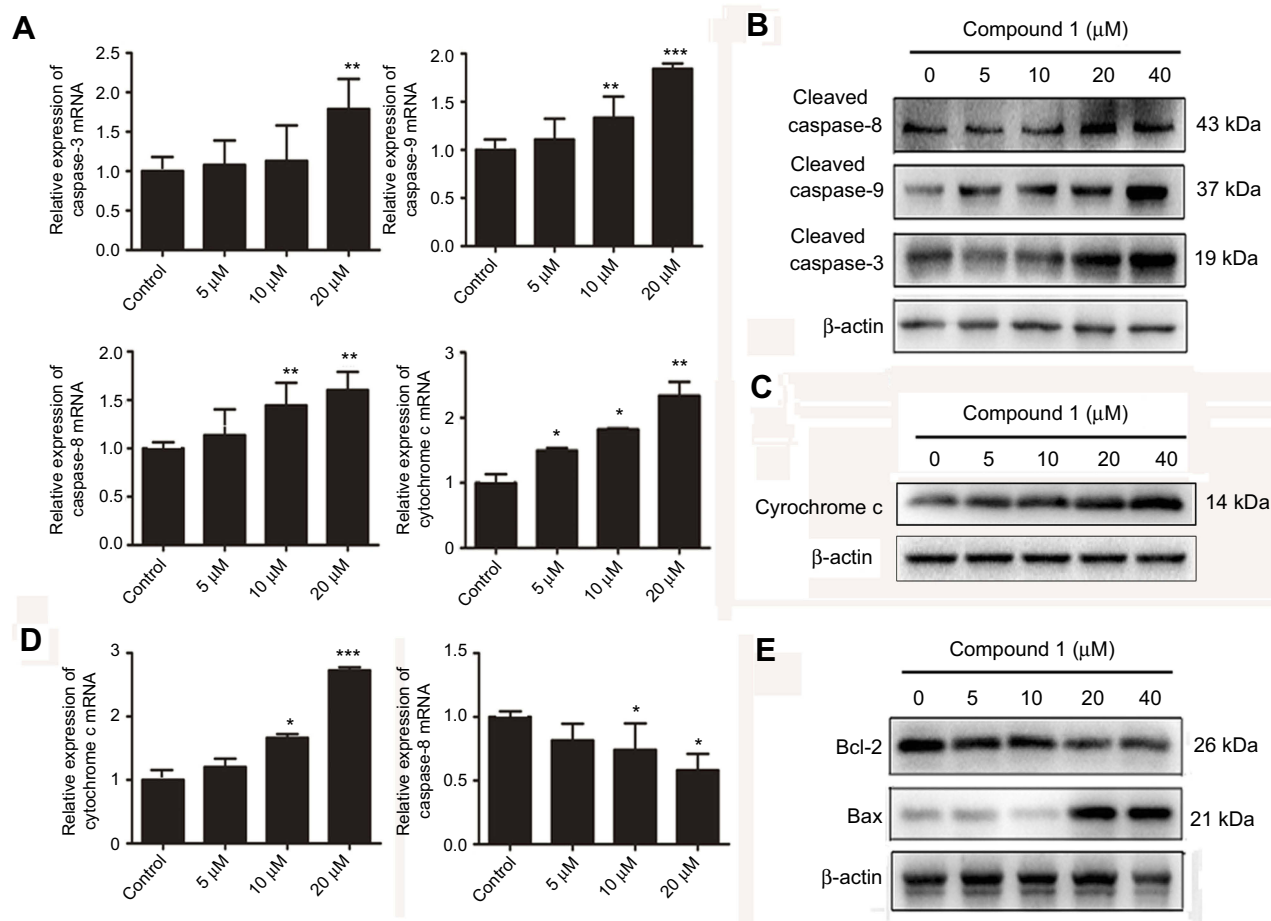


Figure 5 Effects of nudol(1) on apoptosis regulators.

Notes: (A) The mRNA expression of caspase-3, 8, and 9 and cytochrome c in U2OS cells upon treatment of nudol(1) was analyzed after 48 hrs. (B, C) U2OS cells were treated with indicated concentrations of nudol(1) for 48 hrs, and activities of caspase-3, 8, 9 and cytochrome c were detected by Western blotting. (D and E) The mRNA and protein expression of Bax and Bcl-2 were examined by real-time PCR and Western blotting, respectively. Data were represented as mean \pm SD (n=3). * P <0.05, ** P <0.01, *** P <0.001 vs control cells.

Nudol(1) inhibited the mobility of OS cells

We further examined whether nudol(1) played a role in the migration of osteosarcoma cells, and wound-healing assay was then performed. The results showed that nudol(1) could effectively prevent U2OS cells from entering the wounded area (Figure 6A and B), and the cells treated with nudol(1) for 24 hrs demonstrated better effect than control, indicating that nudol(1) was able to efficiently inhibit cell migration. Meanwhile, wound-healing assays were used to evaluate the migration of MG63 cells that were treated with different dosages of nudol(1). The results showed that nudol(1) could also suppress migration of MG63 cells effectively (Figure S3). In addition, we analyzed the effects of nudol(1) on the expression of genes involved in U2OS cell migration. The data indicated

that the expression of MMP2 and MMP9 decreased significantly in the treated group. On the contrary, the expression of genes that suppress migration, such as TIMP1 and TIMP2, increased dramatically (Figure 6C).

Discussion

Osteosarcoma is an aggressive cancer in the skeletal system mostly diagnosed in juveniles. The high mortality rate associated with osteosarcoma indicates that the current available treatments, such as surgical resection and chemotherapy²⁷ are far from satisfying. Therefore, it is necessary to develop new therapeutic agents to treat osteosarcoma effectively.²⁸ In this study, five phenanthrene derivatives (1–5) were obtained from a traditional Chinese herb *D. nobile*, and their growth inhibitory activities against MG63 and U2OS cell lines were investigated

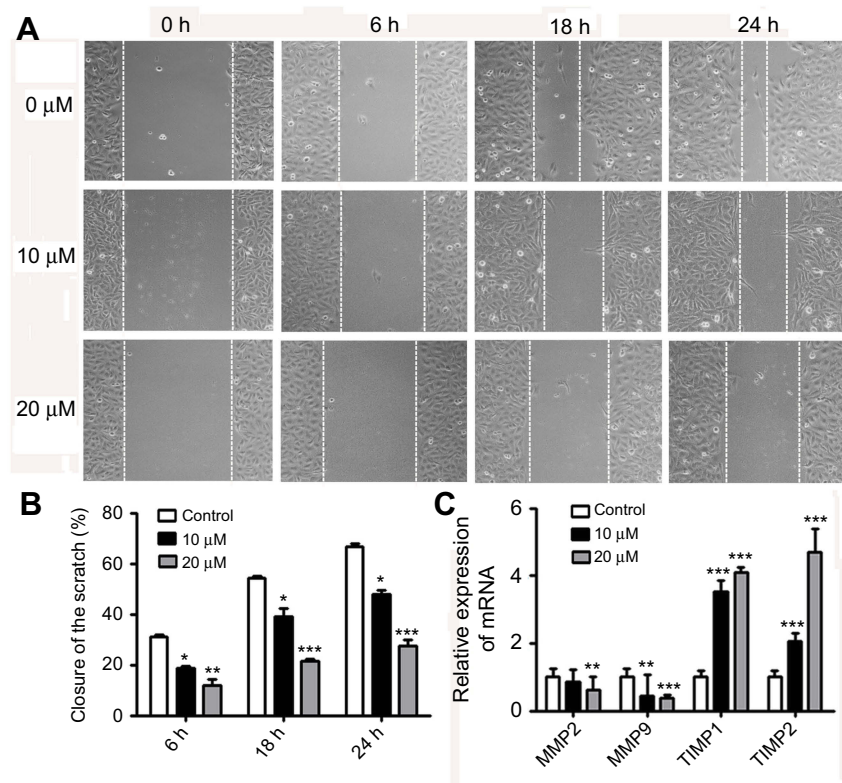


Figure 6 Nudol(1) suppressed migration of U2OS cells.

Notes: (A) Cells were treated with various doses of nudol(1) for 0, 6, 18, and 24 hrs, and the migratory behavior was determined by wound-healing assay. (B) The wound distance of migration was calculated. (C) Real-time PCR analysis for MMP2, MMP9, TIMP1, and TIMP2 in nudol(1)-treated cells. Data were represented as mean \pm SD (n=3). * P <0.05, ** P <0.01, and *** P <0.001 vs control.

by MTT assay. The results indicated that treatment of nudol(1) could significantly decrease the cell viability compared to the control group at 24, 48, and 72 hrs, respectively. In addition, the viability effect of nudol(1) in other cells such as MDA-MB-231, MCF-7, and A549 cells was also confirmed by MTT assay. These results demonstrated that the U2OS cells were more sensitive to nudol(1) treatment, whereas other cell lines exhibited less response. Our present work demonstrated that nudol(1) inhibited human osteosarcoma cells growth by at least partially cell cycle arrest, apoptosis induction, and migration inhibition. We firstly found that treatment of nudol(1) inhibited the viability of U2OS cells by enhancing the cell cycle arrest in the G2/M phase. As CDKs play a key role in the controlling of cell proliferation through maintaining of cell cycling,²⁹ we then examined the expression of several major CDKs and identified nudol(1) as a good suppressor of them. To further illustrate the mechanism, p21 which is a critical regulator of cell cycle was detected.³⁰ As we predicted, the expression of p21 was obviously increased upon treatment of nudol(1), which

was further confirmed by examination of the cell cycle-related proteins CDK1/cyclin B1. In addition, the retinoblastoma tumor suppressor protein (Rb) might contribute to regulating multiple critical cellular activities in preventing tumor, including the cell cycle arrest.^{31,32}

Therefore, the phosphorylation level of Rb (p-Rb) was also tested in nudol(1)-treated U2OS cells and was demonstrated to decrease significantly.

Apoptosis serves as a pivotal role in tumor formation and treatment response.³³ We found that nudol(1) induced apoptosis of U2OS cells in a dose-dependent way, as evidenced by flow cytometry analysis and DAPI staining. Apoptosis is a tightly regulated process under the control of several signaling pathways such as the caspase pathway.³⁴ Activation of caspase-3 plays a central role in the initiation of apoptosis, which requires the activation of initiator caspase-8 or 9.³⁵ From our acquired data, the exposure of U2OS cells to nudol(1) caused the cleavage and activation of caspase-3, 8 and 9 in a dose-response manner. On the other hand, apoptotic stimuli may promote the release of cytochrome c from the mitochondria to the cytoplasm, which could be inhibited by

anti-apoptotic protein Bcl-2.³⁶ Meanwhile, pro-apoptotic protein Bax is able to decrease the inhibitory effect of Bcl-2 on the release of cytochrome c.^{37,38} The release of cytochrome c, in turn, results in the cleavage of pro-caspase-9. Activation of caspase-9 can then go on to activate caspase-3, which triggers apoptosis.³⁹ Our results showed that nudol(1) significantly enhanced the expression of cytochrome c and Bax while reduced Bcl-2 in U2OS cells. Thus, these results demonstrated that the caspase-dependent pathway plays a pivotal role in the apoptosis induced by nudol(1).

Moreover, we found that the migration of U2OS cells was greatly inhibited by treatment of nudol(1). It is well known that cancer invasion and metastasis are a complicated multi-step process involving numerous effects or molecules. The degradation of the extracellular matrix is an essential step in cancer invasion and metastasis.⁴⁰ Matrix metalloproteinases had been verified to degrade almost all extracellular matrix components.⁴¹ Therefore, the homeostatic expression of MMP and their inhibitors TIMP was detected in nudol(1)-treated U2OS cells. Our data demonstrated that nudol(1) could suppress the mRNA level of MMP-2 and MMP-9, and on the contrary, promote the expression of TIMP1 and TIMP2 that suppress migration, which revealed an interesting mechanism on how nudol(1) inhibited cell migration.

In summary, nudol(1) is a natural phenanthrene derivative from the Chinese herb *D. nobile*, the effects and potential molecular mechanisms of nudol(1) were investigated for the first time in human osteosarcoma cells. Our data showed that compound nudol(1) was able to significantly inhibit cell growth, cause G2/M cell cycle arrest, induce cell apoptosis and suppress migration of OS cells. Taken together, the current work identified nudol(1) as a potential lead compound for the development of future osteosarcoma chemotherapies.

Acknowledgments

This research work was financially supported by the National Natural Science Foundation of China (Nos. 31501104, 81402820), the Young Taishan Scholars Program (No. tsqn20161037), Natural Science Foundation of Shandong Province (No. JQ201721), Shandong Talents Team Cultivation Plan of University Preponderant Discipline (No. 10027).

Author contributions

All authors contributed to data analysis, drafting and revising the paper, gave final approval of the version to be published, and agree to be accountable for all aspects of the work.

Disclosure

The authors report no conflicts of interest in this work.

References

- Mirabello L, Troisi RJ, Savage SA. Osteosarcoma incidence and survival rates from 1973 to 2004: data from the surveillance, epidemiology, and end results program. *Cancer*. 2009;115:1531–1543. doi:10.1002/cncr.24121
- Bielack SS, Kempf-Bielack B, Delling G, et al. Prognostic factors in high-grade osteosarcoma of the extremities or trunk: an analysis of 1,702 patients treated on neoadjuvant cooperative osteosarcoma study group protocols. *J Clin Oncol*. 2002;20:776–790. doi:10.1200/JCO.2002.20.3.776
- Kawano M, Tanaka K, Itonaga I, Ieda S, Iwasaki T, Tsumura H. microRNA-93 promotes cell proliferation via targeting of PTEN in osteosarcoma cells. *J Exp Clin Oncol*. 2015;34:76. doi:10.1186/s13046-015-0192-z
- Zhang Y, He Z, Duan Y, et al. Does intensified chemotherapy increase survival outcomes of osteosarcoma patients? A meta-analysis. *J Bone Oncol*. 2018;12:54–60. doi:10.1016/j.jbo.2018.04.001
- Wang L, Yang L, Lu Y, et al. Osthole induces cell cycle arrest and inhibits migration and invasion via PTEN/Akt pathways in osteosarcoma. *Cell Physiol Biochem*. 2016;38:2173–2182. doi:10.1159/000445573
- Ng TB, Liu J, Wong JH, et al. Review of research on *Dendrobium*, a prized folk medicine. *Appl Microbiol Biot*. 2012;93:1795–1803. doi:10.1007/s00253-011-3829-7
- Zhang Y, Wang H, Wang P, Ma C, He G, Rahman MR. Optimization of PEG-based extraction of polysaccharides from *Dendrobium nobile* Lindl. and bioactivity study. *Int J Biol Macromol*. 2016;92:1057–1066. doi:10.1016/j.ijbiomac.2016.07.034
- Li Y, Wang CL, Zhao HJ, Guo SX. Eight new bibenzyl derivatives from *Dendrobium candidum*. *J Asian Nat Prod Res*. 2014;16:1035–1043. doi:10.1080/10286020.2014.967230
- Ma GX, Xu GJ, Xu LS, Wang ZT and Kickuchi T. Studies on chemical constituents of *Dendrobium chrysotoxum* Lindl. *Acta Pharm Sin*. 1994;29:763–766.
- Chen KK, Chen AL. The pharmacological action of dendrobine. The alkaloid of *Chin-shih-hu*. *J Pharmacol Exp Ther*. 1935;55:319–325.
- Ng TB, Liu F, Wang ZT. Antioxidative activity of natural products from plants. *Life Sci*. 2000;66:709–723.
- Sun J, Fu X, Wang Y, et al. Erianin inhibits the proliferation of T47D cells by inhibiting cell cycles, inducing apoptosis and suppressing migration. *Am J Transl Res*. 2016;8:3077–3086.
- Li YM, Wang HY, Liu GQ. Erianin induces apoptosis in human leukemia HL-60 cells. *Acta Pharmacol Sin*. 2001;22:1018–1022.
- Gong YQ, Fan Y, Wu DZ, Yang H, Hu ZB, Wang ZT. In vivo and in vitro evaluation of erianin, a novel anti-angiogenic agent. *Eur J Cancer*. 2004;40:1554–1565. doi:10.1016/j.ejca.2004.01.041
- Wang H, Zhang T, Sun W, et al. Erianin induces G2/M-phase arrest, apoptosis, and autophagy via the ROS/JNK signaling pathway in human osteosarcoma cells *in vitro* and *in vivo*. *Cell Death Dis*. 2016;7:e2247. doi:10.1038/cddis.2016.138
- Lee YHR, Park JD, Baek NI, Kim SI, Ahn BZ. In vitro and in vivo antitumoural phenanthrenes from the aerial parts of *Dendrobium nobile*. *Planta Med*. 1995;61:178–180. doi:10.1055/s-2006-958043
- Zhou XM, Zheng CJ, Gan LS, et al. Bioactive phenanthrene and bibenzyl derivatives from the stems of *Dendrobium nobile*. *J Nat Prod*. 2016;79:1791–1797. doi:10.1021/acs.jnatprod.6b00252
- Ma GX, Xu GJ, Xu LS. Inhibitory effects of *Dendrobium chrysotoxum* and its constituents on the mouse HePA and ESC. *J Chin Pharmaceutical Univ*. 1994;25:188–189.

19. Wang TS, Lu YM, Ma GX, et al. In vitro inhibitory activity of Leukemia K562 cells growth by constituent from *Dendrobium chrysotoxum*. *Nat Prod Res Dev*. 1997;9:1–3.
20. Dou C, Han M, Zhang B, Sun L, Jin X, Li T. Chrysotoxene induces apoptosis of human hepatoblastoma HepG2 cells in vitro and in vivo via activation of the mitochondria-mediated apoptotic signaling pathway. *Oncol Lett*. 2018;15:4611–4618. doi:10.3892/ol.2018.7857
21. Bhandari SR, Kapadi AH, Mujumder PL, Joardar M, Shoolery JN. Nudol, a phenanthrene of the orchids *Eulophia nuda*, *Eria carinata* and *Eria stricta*. *Phytochemistry*. 1985;24:801–804. doi:10.1016/S0031-9422(00)84898-0
22. Majumder PL, Sen RC. Pendulin, a polyoxygenated phenanthrene derivative from the orchid *Cymbidium pendulum*. *Phytochemistry*. 1991;30:2432–2434.
23. Majumder PL, Banerjee S. Two stilbenoids from the orchid *Eria flava*. *Phytochemistry*. 1990;29:3052–3055. doi:10.1016/0031-9422(90)87141-G
24. Zhang X, Xu JK, Wang NL, Kurihara H, Yao XS. Antioxidant phenanthrenes and lignans from *Dendrobium nobile*. *J Chin Pharm Sci*. 2008;17:314–318.
25. Radix S, Barret R. Total synthesis of two natural phenanthrenes: confusarin and a regioisomer. *Tetrahedron*. 2007;63:12379–12387. doi:10.1016/j.tet.2007.09.052
26. Réthy B, Kovács A, Zupkó I, et al. Cytotoxic phenanthrenes from the rhizomes of *Tamus communis*. *Planta Med*. 2006;72:767–770. doi:10.1055/s-2006-941505
27. Anninga JK, Gelderblom H, Fiocco M, Kroep JR, Taminiau AH, Hogendoorn PC and Egeler RM. Chemotherapeutic adjuvant treatment for osteosarcoma: where do we stand? *Eur J Cancer*. 2011;47:2431–2445. doi:10.1016/j.ejca.2011.05.030
28. Zhou W, Hao M, Du X, Chen K, Wang G, Yang J. Advances in targeted therapy for osteosarcoma. *Discov Med*. 2014;17:301–307.
29. Mayer EL. Targeting breast cancer with CDK inhibitors. *Curr Oncol Rep*. 2015;17:20–24. doi:10.1007/s11912-015-0443-3
30. Abbas T, Dutta A. p21 in cancer: intricate networks and multiple activities. *Nat Rev Cancer*. 2009;9:400–414. doi:10.1038/nrc2657
31. Burkhart DL, Sage J. Cellular mechanisms of tumour suppression by the retinoblastoma gene. *Nat Rev Cancer*. 2008;8:671–682. doi:10.1038/nrc2399
32. Gao YF, Zhang QJ, Yu Z, Liu SH, Liang J. miR-142 suppresses proliferation and induces apoptosis of osteosarcoma cells by upregulating Rb. *Oncol Lett*. 2018;16:733–740. doi:10.3892/ol.2018.8761
33. Solary E, Dubrez L, Eymin B. The role of apoptosis in the pathogenesis and treatment of diseases. *Eur Respir J*. 1996;9:1293–1305.
34. Thornberry NA, Lazebnik Y. Caspases: enemies within. *Science*. 1998;281:1312–1316.
35. Patel T, Gores GJ, Kaufmann SH. The role of proteases during apoptosis. *Faseb J*. 1996;10:587–597. doi:10.1096/fasebj.10.5.8621058
36. Vaux DL, Cory S, Adams JM. Bcl-2 gene promotes haemopoietic cell survival and cooperates with c-myc to immortalize pre-B cells. *Nature*. 1988;335:440–442. doi:10.1038/335440a0
37. Renault TT, Tejjido O, Antonsson B, Dejean LM and Manon S. Regulation of bax mitochondrial localization by Bcl-2 and Bcl-xL: keep your friends close but your enemies closer. *Int J Biochem Cell Biol*. 2013;45:64–67. doi:10.1016/j.biocel.2012.09.022
38. Czabotar PE, Lessene G, Strasser A, Adams JM. Control of apoptosis by the BCL-2 protein family: implications for physiology and therapy. *Nat Rev Mol Cell Biol*. 2014;15:49–63. doi:10.1038/nrm3722
39. Würstle ML, Laussmann MA, Rehm M. The central role of initiator caspase-9 in apoptosis signal transduction and the regulation of its activation and activity on the apoptosome. *Exp Cell Res*. 2012;318:1213–1220. doi:10.1016/j.yexcr.2012.02.013
40. Chen P, Hu M, Deng X, Li B. Genistein reinforces the inhibitory effect of Cisplatin on liver cancer recurrence and metastasis after curative hepatectomy. *Asian Pac J Cancer Prev*. 2013;14:759–764. doi:10.7314/apjcp.2013.14.2.759
41. Vihinen P, Ala-aho R, Kähäri VM. Matrix metalloproteinases as therapeutic targets in cancer. *Curr Cancer Drug Targets*. 2005;5:203–220.

Drug Design, Development and Therapy

Dovepress

Publish your work in this journal

Drug Design, Development and Therapy is an international, peer-reviewed open-access journal that spans the spectrum of drug design and development through to clinical applications. Clinical outcomes, patient safety, and programs for the development and effective, safe, and sustained use of medicines are a feature of the journal, which has also

been accepted for indexing on PubMed Central. The manuscript management system is completely online and includes a very quick and fair peer-review system, which is all easy to use. Visit <http://www.dovepress.com/testimonials.php> to read real quotes from published authors.

Submit your manuscript here: <https://www.dovepress.com/drug-design-development-and-therapy-journal>